

ELEVENTH EUROPEAN ROTORCRAFT FORUM

Paper No. 46

COMPOSITE MAIN ROTOR BLADE OF PZL-SOKOL HELICOPTER

Stanisław Kamiński

Transportation Equipment Factory "PZL-SWIDNIK"  
Swidnik, Poland.

September 10-13, 1985

London, England.

THE CITY UNIVERSITY, LONDON, EC1V 0HB, ENGLAND

Errata of remarked errors in paper No 46.

Page	No of line from		There is	Should be
	below	above		
46-7		11	... of pylon	... of blade
46-8		4	/see Fig. 2/	/see Fig. 3/
46-8		13	... was close to no-	... was close to 4x no-
46-11	2		- AT DECENT ...	- AT DESCENT
46-11	11		Deçent	Descent

COMPOSITE MAIN ROTOR BLADE OF PZL-SOKOL HELICOPTER

Stanislaw Kamiński, M.Sc., Eng.

Chief Design Engineer

Transportation Equipment Factory "PZL-Swidnik"

Swidnik, Poland.

Introduction to this paper includes some interesting events from the history of composite rotor blades in PZL-Swidnik. The following chapters include the blade cross section structure, blade geometry, and its mass and stiffness distributions. Resonance diagrams, one of them with pylon flexibility included, are given. Surveys of static, dynamic, fatigue and weather ageing tests, the tests on a tied-down helicopter, and the flight tests are also discussed here. Unique dynamic phenomenon of low torsional stiffness blades stall flutter and pylon resonance are discussed in the FLIGHT TESTS chapter.

NOTATION			
R	= rotor radius, meters	V	= helicopter airspeed; km/h
$\Omega$	= rotor angular speed; radians per second	$\delta_T$	= blade tab deflection angle positive for trailing edge up, degrees
$\Omega R$	= rotor tip speed, meters per second	$T_0$	= blade root torsional moment /feathering moment = pitch link load x the arm relative to pitching axis/, Nm
c	= blade chord	$T_1$	= blade section torsional moment at $\bar{r} = 0.595$ , Nm
r	= blade radial coordinate; meters	$M_p$	= pitch housing bending moment approximately in the plane of rotation, Nm
Nm	= Newton per meter = 1 kg x meter <sup>2</sup> x second <sup>2</sup>	$M_t$	= pitch housing bending moment approximately in the thrust plane, Nm
s	= second	$SM_d; SM_u$	= rotor shaft bending moments in rotational coordinate system, suitably 0.6 m and 0.2 m down from the plane of rotation, Nm
$\bar{r} = \frac{r}{R}$	= dimensionless blade radius 0 at the center of the rotor and 1.0 at the tip	$SM_{dIII}$	= 3rd harmonic component of $SM_d$
P	= % per main rotor revolution	N	= rotor r.p.m.
$GI_0$	= torsional stiffness of blade section Nm x m <sup>2</sup>	$N_{nom}$	= nominal rotor r.p.m.
$EI_y$	= bending stiffness of blade section in chordwise plane N x m <sup>2</sup>	p	= blade natural frequency, cycles per minute
$EI_x$	= bending stiffness of blade section in flatwise plane, N x m <sup>2</sup>	min	= minute
$\psi$	= blade azimuth $\psi = \Omega \cdot t$ ; 0 = when the blade is above the helicopter tail boom and increases in the direction of rotation, degrees	OAT	= outside air temperature in flight; °C
t	= time; seconds	H	= flight altitude, meters
$\beta$	= flapping angle of the blade positive for blade axis up; degrees	$TOM$	= helicopter takeoff mass, kg
$\xi$	= lagging angle of the blade positive for blade axis lag; degrees		
$C_H$	= blade airfoil pitching mo- ment coefficient		

INTRODUCTION

The history of PZL-Swidnik composite rotor blades began in 1959. In 1960 the main rotor blades for the SM-4 Latka helicopter were designed and manufactured.

Almost at the same time, composite main rotor blades for the Mi-1 helicopter were designed. They were based on the room temperature curing technology. Some of these blade sets had flown up to 400 hours.

Composite main and tail rotor blades for the Mi-2 helicopter were designed in 1966. Their technology was based on two stage, high temperature curing, preliminarily in 60°C, and then in 150°C. Polish certification for these blades was obtained in 1968, after completion of the full stand, ground, and flight tests program, and then, five sets of these blades were assigned for operation under Aviation Authorities supervision.

So far, we have an almost fifteen-years-long experience with the above blades. At present, several years after manufacturing, some sets of these blades are still in operation on a few PZL-Kania helicopters.

Paralelly, a few types of large, 3, 6, and 8 meters diameter, industrial rotor blades were designed and manufactured on the basis of room temperature technology. After almost twenty years of their operation, no serious problems arose, apart from leading edge and blade paint erosion.

On the basis of the experiences mentioned above, in the preliminary stages of the PZL-Sokol helicopter development it was decided to design and develop composite rotor blades with low torsional stiffness, with no fibre layers angled at 45° to the blade axis.

The risk of development of the low torsional stiffness blades was undertaken on the basis of earlier difficulties in obtaining high torsional stiffness of a composite structure, elastic in its nature, and also because of the qualitative expectation that such a structure design may improve the helicopter performance.

Obviously, the involvement of composite materials such as glass

fibre and fabrics in the design of the blade necessitated the in-house static, fatigue, and environmental tests, which were required for certification, as well, as evaluation of solar heating effect, natural moisture absorption etc. The lightning tests are almost completed by now.

A short survey of static, fatigue, and natural ageing tests made for PZL-Sokol blade qualification is presented here. The unique phenomenon of stall flutter with pylon resonance presence, which appeared in preliminary stages of the PZL-Sokol flight tests, is discussed in a more detailed way.

#### BLADE DESCRIPTION

The main rotor of the PZL-Sokol helicopter consists of four blades with a fully articulated hub.

The basic airfoil of the blade has 440 mm nominal chord NACA 230M, with 16 to 9 per cent thickness from root to tip. Linear twist along the blade length is 10°39'.

The blade consists of a D-front spar, afterbody skins stabilized by a honeycomb core made of glass fabric, and a trailing edge strip. In the outboard area of the blade, the trailing edge skins are stretched out of the nominal chord in order to form 5 per cent trailing edge tabs.

Fig. 1 presents a typical cross section of the blade. Fig. 2 presents blade geometries in particular variants of design. The key structural components of the spar are spanwisely oriented glass fibres and glass fabrics in an epoxy matrix. The fibres are wrapped around a two-hole fastener, so that they form a loop joint of the two, longitudinally oriented, attachment bolts. No torsion plies with 45° fibre orientation are used.

In the outboard area of the blade a leading nose block provides the necessary section balance and in-

tational inertia. The honeycomb core extends from the trailing edge of the spar to the unidirectional blade trailing edge member to support the skin. The skin consists of three plies made of glass fabric with 0°-90° fibres orientation.

Electrical heater mats with the supply wires for the deicing system are also glued to the blade leading edge surface.

The deformable trim tab of the blade is made of duralumin.

Fig. 3 presents blade mass, center of gravity, and elastic centers distribution.

Fig. 4 presents flapwise, chordwise, and torsional stiffness distributions of the blade.

Figs. 5 and 6 present diagrams of natural blade frequencies. The diagram in Fig. 6 includes the influence of pylon flexibility.

#### ULTIMATE AND PROOF TESTS AND OTHER MEASUREMENTS

The static test program consists of the following tests:

1. Static tension tests of the blade - ultimate strength factor equal 4. This load factor includes, beside the basic safety factor equal 2, an extra safety factor equal 1.33, traditionally approved for composites in PZL - Swidnik.
2. Blade ultimate bending tests for the "stop dump" case of flapping hinge.
3. Root end ultimate bending test in flatwise and chordwise directions /with tension/, and ultimate torsion tests /with tension/.
4. Ultimate torsion tests of the whole blade. It should be stressed here that the test resulted in blade failure at torsional moment equal 3670 Nm applied at  $\bar{r} = 0.9$  and blade tip torsional deflection equal to 146°.
5. Tension free ultimate bending tests in chordwise direction in order to determine the root and

attachment strength and buckling strength of the blade trailing edge.

6. Blade tip proof loading in flapwise and chordwise directions.
7. Determination of bending stiffness in both planes and torsional stiffness.
8. Determination of blade tip deflection under own weight.
9. Determination of elastic centers location in typical cross sections of the blade.
10. Determination of mass and center of gravity distribution in typical cross sections of the blade and blade dynamic axis location by cutting the blade into segments and appropriate measurements and calculations.

#### DYNAMIC TESTS

Dynamic tests consisted in leading the blade root end into vibration with a dynamic shaker in order to determine the first, second, and third flapwise natural frequencies and mode shapes, and the first and second torsional natural frequencies and mode shapes.

The test consisted in vibrating the blade sinusoidally and varying the frequencies until the blade natural frequencies were found.

Measurements of the first torsional natural frequency of the blades on an unoperating helicopter in order to consider the influence of control system stiffness and blades coupling through the swash plate were carried out independently.

The lowest results received were as follows:

- 3.1 P for isolated blade torsion vibration tests
- 3.6 P for blade torsion vibration test on an unoperating helicopter /It seems that these measurements were not correct/

## FATIGUE TESTS

In the course of the Mi-1 and Mi-2 helicopters prototype blades development; the coupon fatigue tests were conducted in order to build Wöhler's and Haigh's diagrams which are not included in current literature. On this basis the fatigue tests for the PZL-Sokol helicopter blades were conducted on 12 segments of prototype blades only. Two blade sections and root segments involving root retention fitting were examined. For each of these two blade sections two segments for each bending plane were tested. Identical tests were carried out up to  $50 \times 10^6$  cycles on each load level.

There were three load levels; with tensile centrifugal force. Each subsequent level of bending loads differed from the preceding one by 50 per cent at constant tensile force.

In the course of further tests the number of each type of blade segments is planned to be increased to 4 + 6. It proved impossible to damage the blade spar in the course of the above tests.

A few blade segments that passed the above tests underwent some extra fatigue tests at the temperature of  $80^{\circ}\text{C}$ , and such tests with an operating deicing system. /This system operated at limited electrical power supply/. An appropriate temperature in the test chamber was kept by lamps radiating heat at both upper and lower skins of the blade segments.

## WEATHERING TESTS

In order to check the influence of a long-lasting exposition to the weather conditions upon the glass-epoxy composite strength; a lot of small samples were produced; and subjected to static, tension, compression, and bending tests.

The tests of particular sets of

samples were carried out after 2 + 3 years of them being exposed to weathering. Considerable decrease in the strength was noted in case of the unpainted samples. In case of the samples painted with an epoxy paint this decrease was considerably smaller. The greatest decrease and scatter of strength was revealed by samples subjected to compression tests.

Five Mi-2 helicopter composite blades were also exposed to weathering. These blades were subjected to stiffness measurements and ultimate tension tests each three years of natural ageing. The tests on small samples were held up to 10 years of natural ageing; and whole blades up to 15 years. The measurements of stiffness and ultimate tension tests of aged blades after 15 years of natural ageing revealed satisfactory static strength; and so, they were approved for operation for such a period of time.

The conclusions drawn from the above tests were utilized in designing the PZL-Sokol blades, which are made of almost the same materials.

## LIGHTNING TESTS

These tests are being carried out by Warsaw Institute of Technology; and are almost completed by now.

All these tests gave basis for approving the blades for tests on a tied-down helicopter; and then for flight tests; with a suggestion of operation on a "FAIL SAFE" principle.

## TIED-DOWN HELICOPTER TESTS

These tests began with the measurements of loads in the chosen blade sections; rotor hub; rotor shaft; and swash plate - at full ranges of collective and cyclic pitch and main rotor r.p.m. Flutter margin had been checked earlier by 3 per cent displacement of the blade dynamic axis in direction to the trailing edge. It had been done by placing appropriate

weights on the blade trailing edge at  $0.7 \pm 0.75$  of the blade radius.

Three different types of blade geometries were tested. /See Fig. 2/. They differed in tips and location of trailing tabs.

At the beginning variant A blades were tested. These blades caused a heavy vibration of a tied-down helicopter, which could be decreased by changing the helicopter burden in order to detune it from the main frequency transmitted through the hub, i.e. 4 P. Considerable increase in vibration was noticed, particularly at high collective and cyclic pitch, and at decreasing the main rotor r.p.m.

A similar phenomenon, but considerably more intense, was observed on a full scale transmission test stand.

In spite of an alarming behaviour of a tied-down helicopter, it was decided to test the blades in flight. It was assumed here, that the characteristics of the pylon - rotor system is different in flight than when tied down or on a transmission stand. /See chapter concerning tests in flight/.

The endurance tied-down tests were carried out for 1000 hrs. Each individual test lasted for 200 hrs. The tests are to be continued up to 1500 hrs. total.

During the first 150 hrs. of a tied-down helicopter tests small but essential changes in blade construction were being tested. The variant C blades underwent the tests after first 200 hrs of testing. Test load measurements in particular operational stages of 200 hrs. test were carried out after the first 100 hrs. of helicopter operation and then before and after each 200 hrs. period.

#### FLIGHT TESTS.

A short maiden flight at limited speed was performed on the helicop-

ter which was to be used for tied-down tests, with tabless blades, tapered at the tips. Piloting and handling of the helicopter was generally good, but, from time to time, some short waves of vibration were observed in the fuselage even in hover. The measurements of mean loads in the collective control system revealed too high values. It was then decided that the Variant A blades, Fig. 2, are to be tested on the first flight prototype helicopter. The variant A blades had 9 per cent tabs at  $\bar{r} = 0.29 \pm 0.7$ , and angles of deflection  $\delta_T = 15^\circ \pm 4^\circ$  upward to the nominal airfoil chords.

First flights with the variant A blades revealed too high a helicopter vibration, high hub and control system loads within the airspeed range from 30 to 120 km/h, and unsafe values at the airspeeds over 120 km/h. Shortening the tabs from 9 to 5 per cent resulted in considerable improvement, but did not solve the whole problem. There were also certain difficulties in blade tracking.

The records of blade torsional moments  $T_1$  at  $\bar{r} = 0.595$  and feathering moment  $T_0$  versus blade azimuth are shown in Figs. 7 and 8 for hover and level flight at  $V = 80$  km/h.

A hypothesis had been put forward that the self-exciting vibration provoked by self-control of hydraulic boosters from gear box body vibration, may be responsible for these problems. In order to solve them, the range of hydraulic boosters insensitivity had been increased. It appeared, however, that the problem remained unsolved. The pilot had again had some problems in controlling the helicopter, even in hover.

The situation was critical - there had been a helicopter, but there were no possibility to fly it. The members of the top design team

were rather depressed and crestfallen. Various hypotheses were being put forward. Checking them did not give any satisfactory explanation of the phenomenon.

Nevertheless it was sure that there is some self-excited vibration on the helicopter. The question remained: by what channel and where from the energy is transmitted to the helicopter systems supporting its vibration?

In this critical moment, the chief designer put forward a seemingly incredible hypothesis: at very low forward speeds, and sometimes in hover, there appears a strong stall flutter phenomenon on the rotor blades. This conclusion had been drawn from the records of blade torsional moments  $T_1$  and  $T_0$  - Figs. 7 and 8, where the notation S denotes suspected complete cycle of moment stall. The records of torsional moments  $T_1$  at  $\bar{r} = 0.595$ ; in Figs. 7a and 8b, show an unstable behaviour of the outboard blade part and it could be suspected that several stall cycles exist there.

The hypothesis was confirmed by  $T_1$  waveform, Fig. 8c, where evident calmness of the waveform, and a smaller amplitude are observed. Handling of the helicopter in descent, from the very beginning of the flight tests; was sufficiently good and vibration was kept at a low level.

It is worth to mention that the suspected moment stall spikes in the feathering moment records  $T_0$  appeared as cycles of torsional response well within the basic 1P waveform, Fig. 8a.

After receiving the above mentioned results, the work was concentrated upon the blade. At the same time the solution for the pylon resonance problem was sought. Among other things, a pendulum vibration absorber, mounted on a hub head; for the 3rd excitation frequency in the rotation plane was constructed.

Suspecting that the main reason for the stall flutter was the im-

proper characteristics of the airfoil aerodynamic moment coefficient at  $\bar{r} = 0.75 \div 1.0$ ; and the decrease in  $C_{Lmax}$  of the airfoil at  $\bar{r} = 0.29 \div 0.695$  in result of the trailing edge tabs deflected upwards,

the tabs at  $\bar{r} = 0.29 \div 0.695$  were removed, and 7.5 per cent c chord tabs in the chord plane at  $\bar{r} = 0.75 \div 1.0$  were introduced. The tabs formed extensions of the catalogue airfoil chords except for one tab segment at  $\bar{r} = 0.867 \div 0.925$  deflected  $8^\circ$  upwards. In result of these changes; variant B blade geometry was received, Fig. 2.

With this blade variant installed the helicopter arrived at the assumed for the test airspeed of 200 km/h, revealing considerably lower vibration. It became clear that the trailing edge tabs constitute an important factor; which influences the level of helicopter vibration. This blade could also be easily trackable. An experimental flight was also performed; with all the above mentioned tabs deflected  $4^\circ$  upwards - the level of vibration increased considerably again; so the tab angles were converted to the former ones.

However; because of the high mean load on the swash plate; it was decided to try the variant C blades /Fig. 2/; with tapered tips, and similarly arranged tabs; but 5 per cent c long.

#### Variant C<sup>II</sup> blade geometry

Since a set of blades, very similar to variant C, was prepared in the meantime; it was decided to perform experimental flights with these blades. These blades were denoted as variant C<sup>II</sup>.

This set of blades had 7.5 per cent C tabs arranged identically as variant B; but had no tab at  $\bar{r} = 0.925 \div 1.0$ .

To more detune the fuselage from the main excitation frequency 4P; 100 kgs weight was installed onto



the top of the main rotor shaft;

The helicopter equipped in this way, with the variant C<sup>II</sup> blades installed, reached 260 km/h maximum level speed. The records of selected main rotor parameters are presented in Figs. 9, 10, and 11. They show that the characteristic stall spikes appear at  $V = 260$  km/h, at rotor tip speed  $\Omega R = 212.5$  m/s /Fig. 11a/, and confirm the presence of pylon resonance with 3rd harmonic excitation frequency in chordwise plane /Fig. 11b/, and with 9th harmonic excitation frequency in flapwise plane, /Fig. 11c/. /See also Fig. 6/. It must be also noted that the 3rd harmonic of shaft bending moment considerably increases, together with the appearance of characteristic stall spikes on  $T_0$  plotting. It can be seen in Figs. 10d and 11d, where it is almost doubled.

Similarly, it happens with the flapping angles, Figs. 10f and 11f.

Fig. 12 presents feathering moments  $T_0$  for variant C<sup>II</sup> blades with all the 5 per cent tabs deflected  $4^\circ$  up. /At weight of 6100 kgs/ It may be observed that these characteristic spikes appear at  $V = 220$  km/h, and rotor tip speed  $\Omega R = 208$  m/s, /Fig. 12a/, and they disappear with rotor tip speed increase to  $\Omega R = 221$  m/s, /Fig. 12b/. They appear again with the helicopter airspeed increase up to  $V = 260$  km/h, /Fig. 12c/.

In each case the stall spikes appeared, the helicopter vibration increased. We can say that the more intense spikes, the more intense the helicopter vibration. Nevertheless, the general opinion of the pilot, as well as the measurement records taken at  $\Omega R = 220$  m/s, were rather positive.

Comparison of the results of flight tests of variants B and C<sup>II</sup> blades showed that the swept back tapered tip gives higher mean loads on control system, both in collective and cyclic pitch, increasing the mean and particularly first harmonic of the feathering moment.

### Variant C of blade geometry

Variant C blade constitutes the final configuration of PZL-Sokol main rotor blade. The 5 per cent tabs at  $\bar{x} = 0.753 \pm 1.0$  form extensions of upper and lower skins of the blade and coincide with the chords of nominal airfoils, except at  $\bar{x} = 0.867 \pm 0.925$ , where the tab segment is deflected  $4^\circ$  upward. Additional 9 per cent a tab at  $\bar{x} = 0.695 \pm 0.752$  is made of duralumin and is used for aerodynamic blade tracking.

After introduction of the above blades, and a hub mounted, Salomon type, pendulum vibration absorber for 3rd harmonic frequency in the rotation plane, the helicopter reached the level speed over 260 km/h, with  $\Omega R = 220$  m/s.

It appeared that at  $\Omega R = 210$  m/s the helicopter may reach the airspeed of 240 km/h, and, at  $\Omega R = 200$  m/s 180 km/h, the level of vibration remaining low.

It was found out that if  $\Omega R$  is not increased above these values it leads to increased vibration and characteristic spikes in feathering moment records  $T_0$ , and increase of swash plate alternate moments, especially longitudinal, in cyclic control, which, as a whole, may be treated as the evidence for stall flutter.

The records of feathering moment  $T_0$  for final configuration of the helicopter with variant C blades are shown in Fig. 13. Fig. 14 presents the changes in swash plate control loads versus helicopter airspeed.

For economical reasons, in result of flight tests, it was decided to preserve the possible range of  $\Omega R = 200 \pm 220$  m/s, which had been assured earlier by appropriate design of the powerplant electro-hydraulic fuel control system.

Allowable rotor tip speeds versus helicopter airspeed and density altitudes are presented in Fig. 15.

## CONCLUDING REMARKS

1. The main reason for the negative dynamic phenomena on the PZL-Sokol helicopter in the preliminary stage of flight tests was the stall flutter of the main rotor blades, which appeared at very low airspeeds, and on a tied-down helicopter, as well as on a natural transmission test stand, at high collective and/or cyclic pitch. The second but not less important reason was that the so-called pylon resonance frequency was close to nominal main rotor r.p.m. "Curing" the problem by elimination of pylon resonance only would be a passive method, which would improve neither the blade operation nor the helicopter performance. It also would not sufficiently decrease the hub and swash plate loads. An active method of dealing with the problem was to remove the stall flutter. It decreased the loads on the hub and swash plate, the helicopter vibration, and improved its performance. Nevertheless, with no hub mounted vibration absorber, it would be difficult to talk about a good helicopter.
2. It is particularly important for the blade with low torsional stiffness to appropriately select the aerodynamic characteristics of the airfoils, especially  $C_{L\alpha}$ .
3. Swept back tapered tip appeared to be less effective than tapered tip in the PZL-Sokol blade configuration. It was responsible for the increase of mean and 1st harmonic feathering moments. However, a positive feature of this tip should also be mentioned here - it increases the blade pendulum flutter margin.
4. Upward deflection of the airfoil trailing edge tabs in the PZL-Sokol blade configuration decreases the stall flutter margin, increases the hub and control system loads, and helicopter vibration.
5. The PZL-Sokol main rotor blade, being a low torsional stiffness blade has some features of the Aeroelasti-

cally Conformable Rotor Concept /ACRC/ blade, as the airfoils pressure centers are considerably behind the elastic centers. /See Fig. 2/

6. In the development of the ACRC blade elimination of the stall flutter phenomenon may appear a serious problem, which, as it seems, has not been discussed so far.

## REFERENCES

1. F.O. Carta, et al., Determination of airfoil and rotor blade dynamic stall response, Journal of the American Helicopter Society, Vol. 18, No. 4, 1973.
2. R.H. Blackwell, et al., Wind tunnel evaluation of aeroelastically conformable rotors, Journal of the American Helicopter Society, Vol. 26, No. 2, 1981.
3. R.H. Stroub, et al., Rotor blade tip shape effects on performance and control loads from full-scale wind tunnel testing, Journal of American Helicopter Society, Vol. 24, No. 5, 1979.
4. J.M. Martin, et al., An experimental analysis of dynamic stall on an oscillating airfoil, Journal of the American Helicopter Society, Vol. 19, No. 1, 1974.
5. R.H. Blackwell, et al., The aeroelastically conformable Rotor Concept, Journal of the American Helicopter Society, Vol. 24, No. 4, 1979.
6. F.J. Tarzanin, Jr., Prediction of Control Loads Due to Blade Stall, Journal of the American Helicopter Society, Vol. 17, No. 2, 1972.
7. W. Johnson, et al., On the mechanism of dynamic stall, Journal of the American Helicopter Society, Vol. 17, No. 4, 1972.
8. R. Geoffrey Benson, et al., Influence of airfoils on stall flutter boundaries of articulated helicopter rotors, Journal of the American Helicopter Society, Vol. 18, No. 1, 1973.

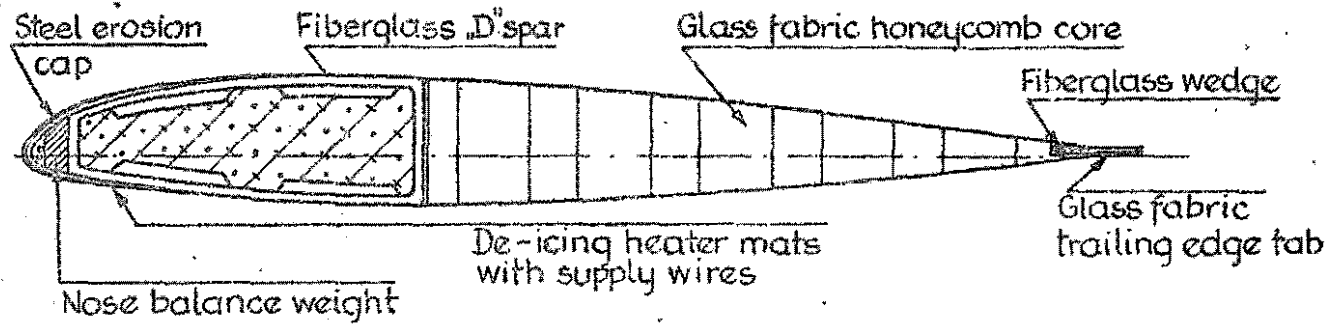


Figure 1. Typical outboard section of blade variant „C” geometry.

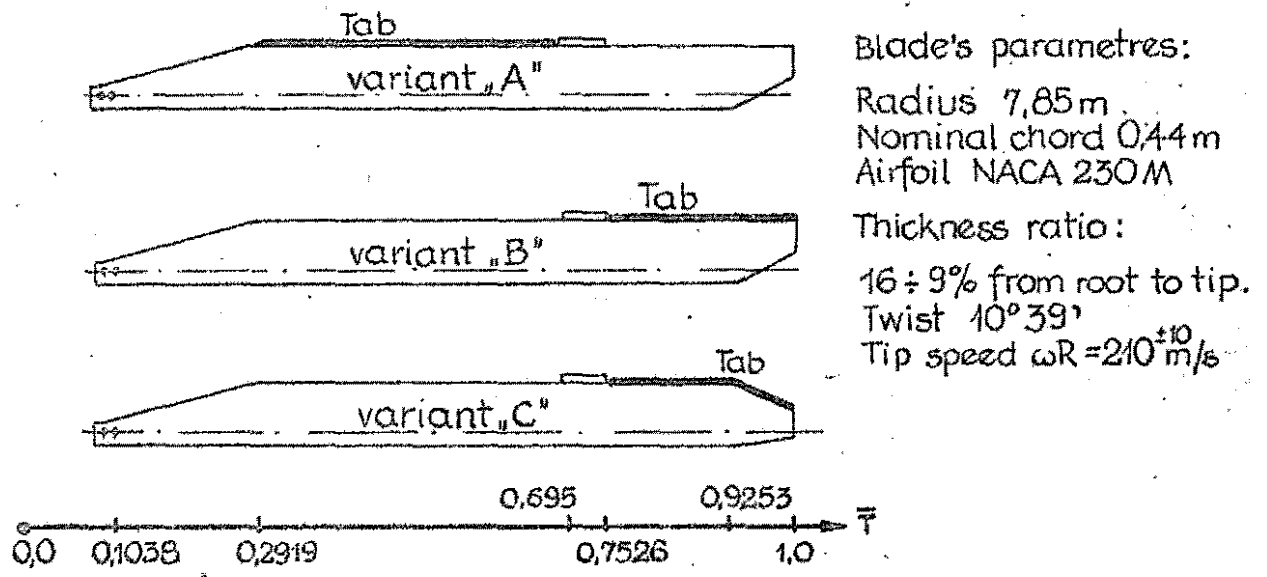


Figure 2. Rotor blade geometries.

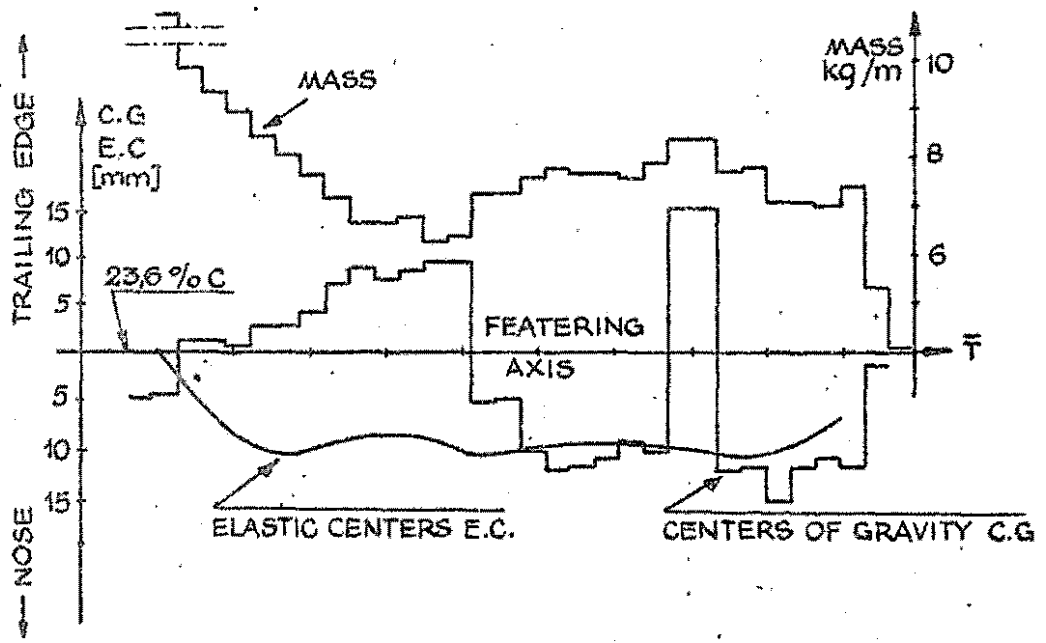


Figure 3. Mass, centers of gravity and elastic centers distributions.

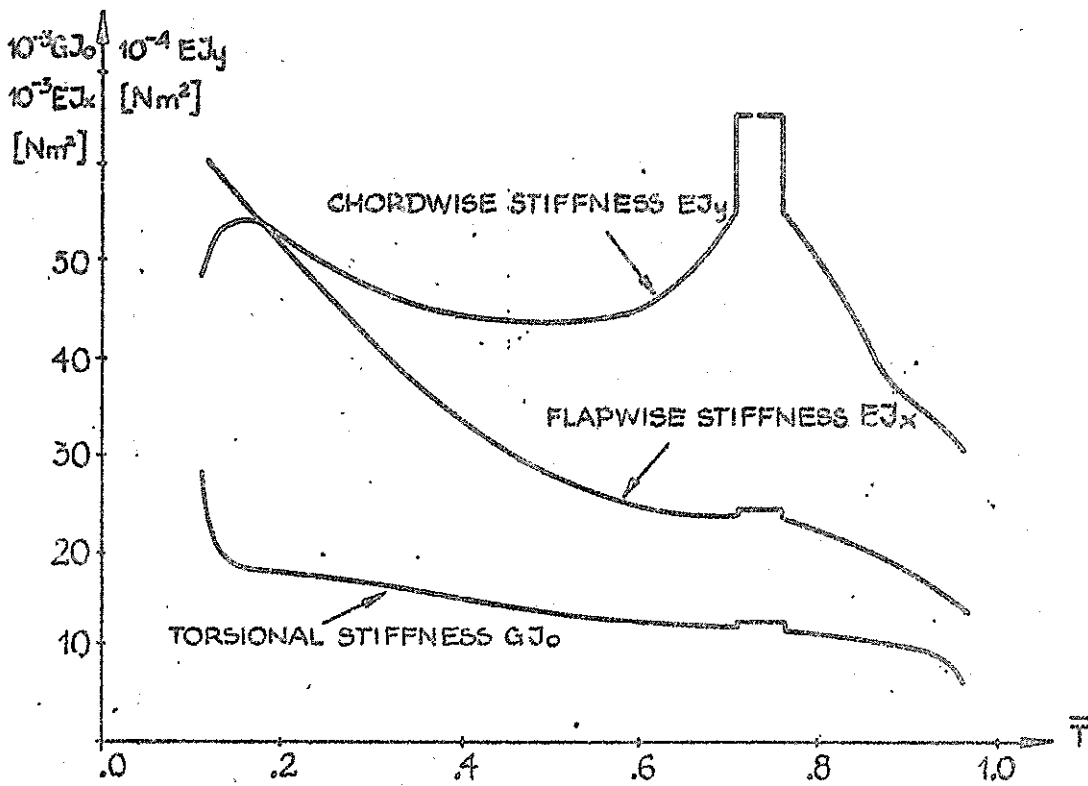


FIGURE 4. FLAPWISE AND CHORDWISE BENDING STIFFNESS AND TORSIONAL STIFFNESS DISTRIBUTIONS.

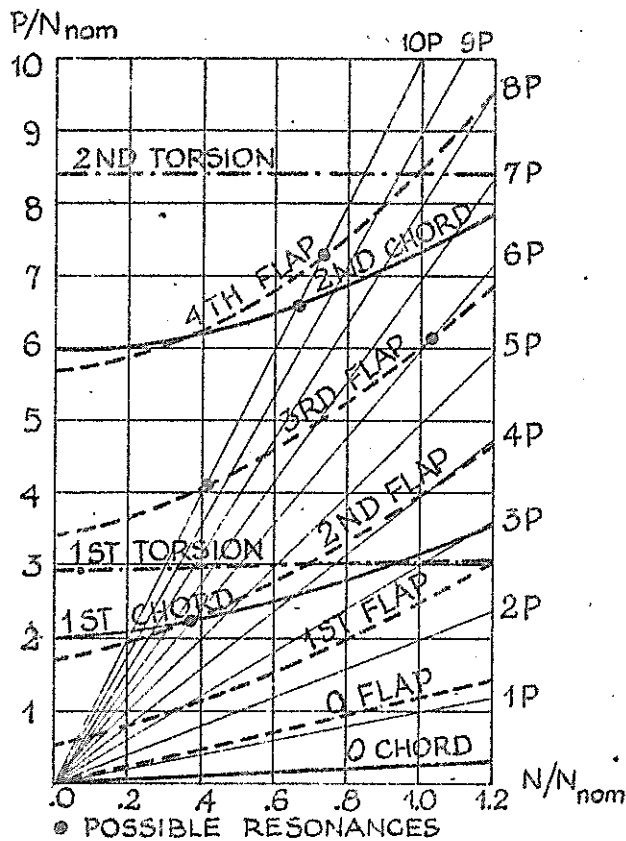


FIGURE 5. CALCULATED BLADE FREQUENCY DIAGRAM WITHOUT THE INFLUENCE OF PYLON FLEXIBILITY. HUB REACTIONLESS MODES.

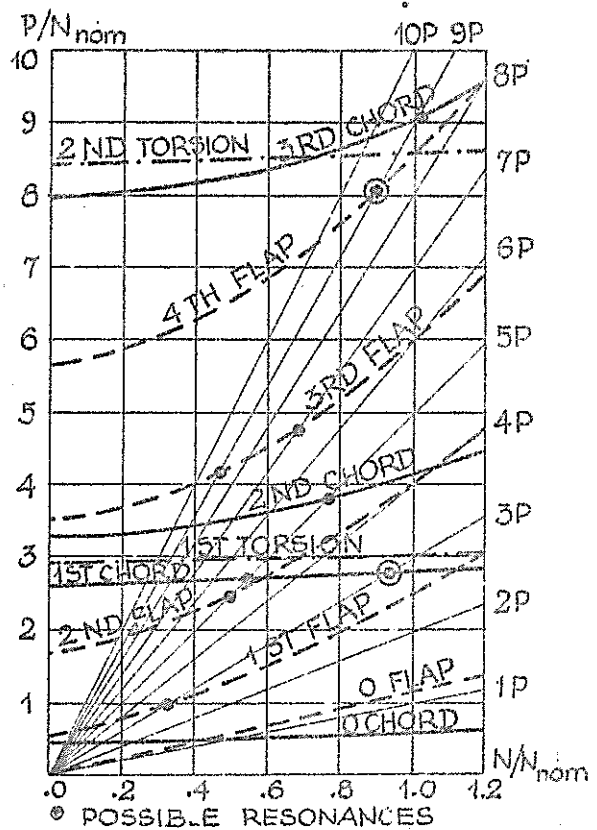


FIGURE 6. CALCULATED BLADE FREQUENCY DIAGRAM WITH THE INFLUENCE OF PYLON FLEXIBILITY. HUB REACTION CYCLIC MODES.

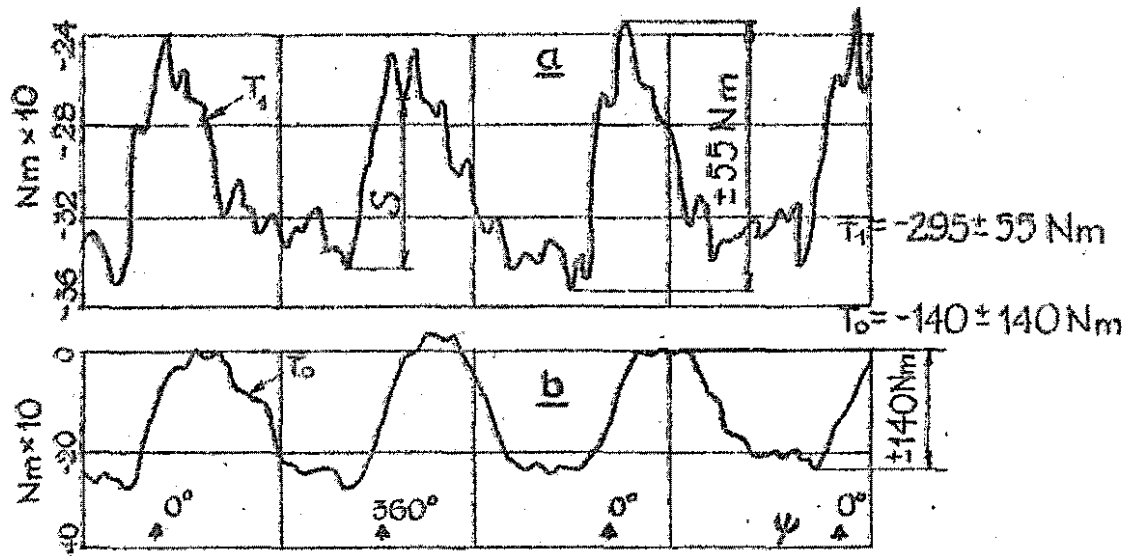


FIGURE 7. RECORDS OF TORSIONAL MOMENTS OF THE BLADE  $T_1$  AT  $F = 0,595$  AND  $T_0$  AT ROOT, IN ONE OF HOVERS.  $\Omega R = 240 \text{ m/s}$ .  $TOM = 5410 \text{ kg}$  BLADES - VARIANT A.

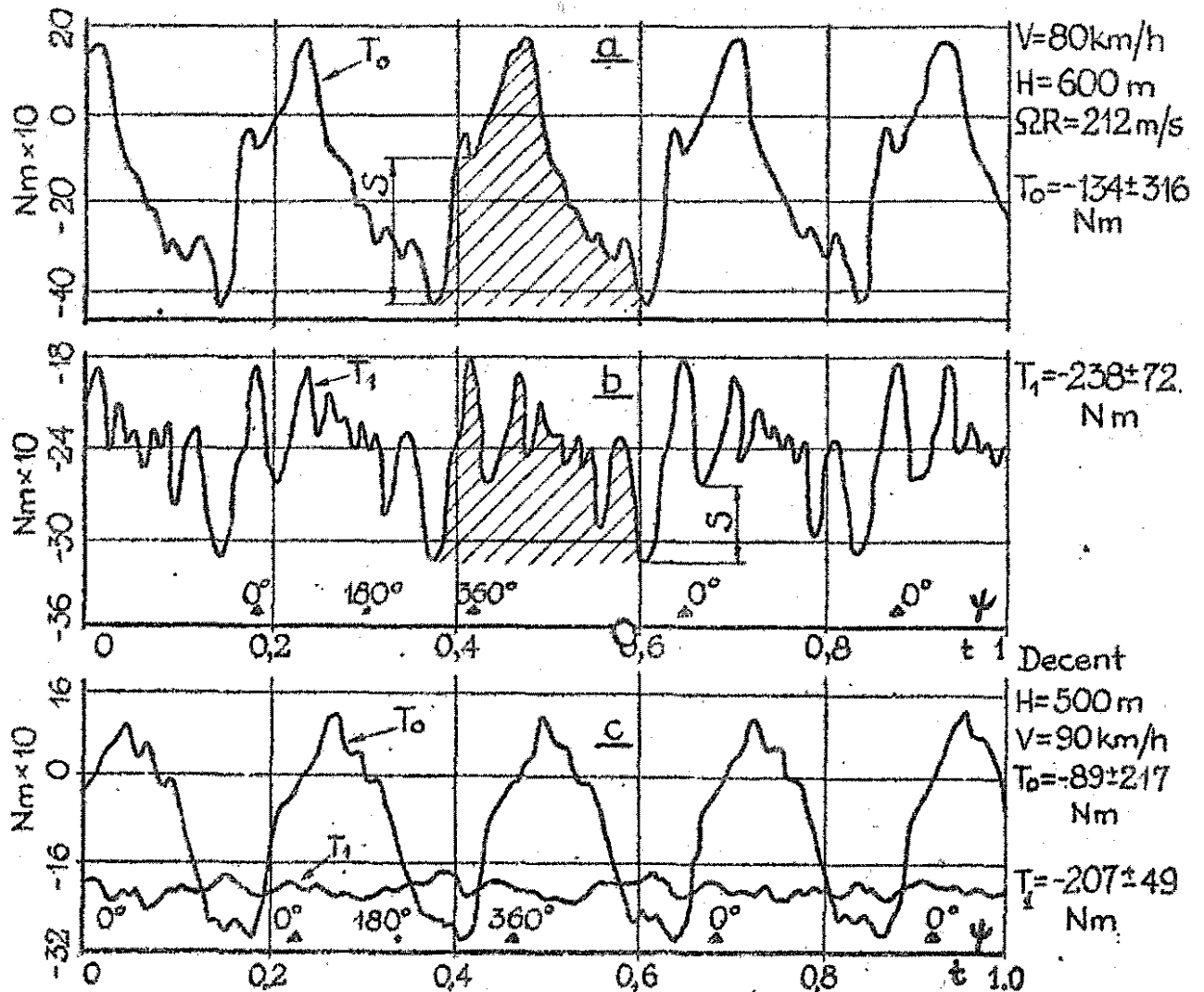


FIGURE 8. RECORDS OF TORSIONAL MOMENTS OF THE BLADE: a AND b - AT LEVEL FLIGHT WITH  $v = 80 \text{ km/h}$  c - AT DECENT WITH  $v = 90 \text{ km/h}$ . BLADES - VARIANT A.  $TOM = 5410 \text{ kg}$ .

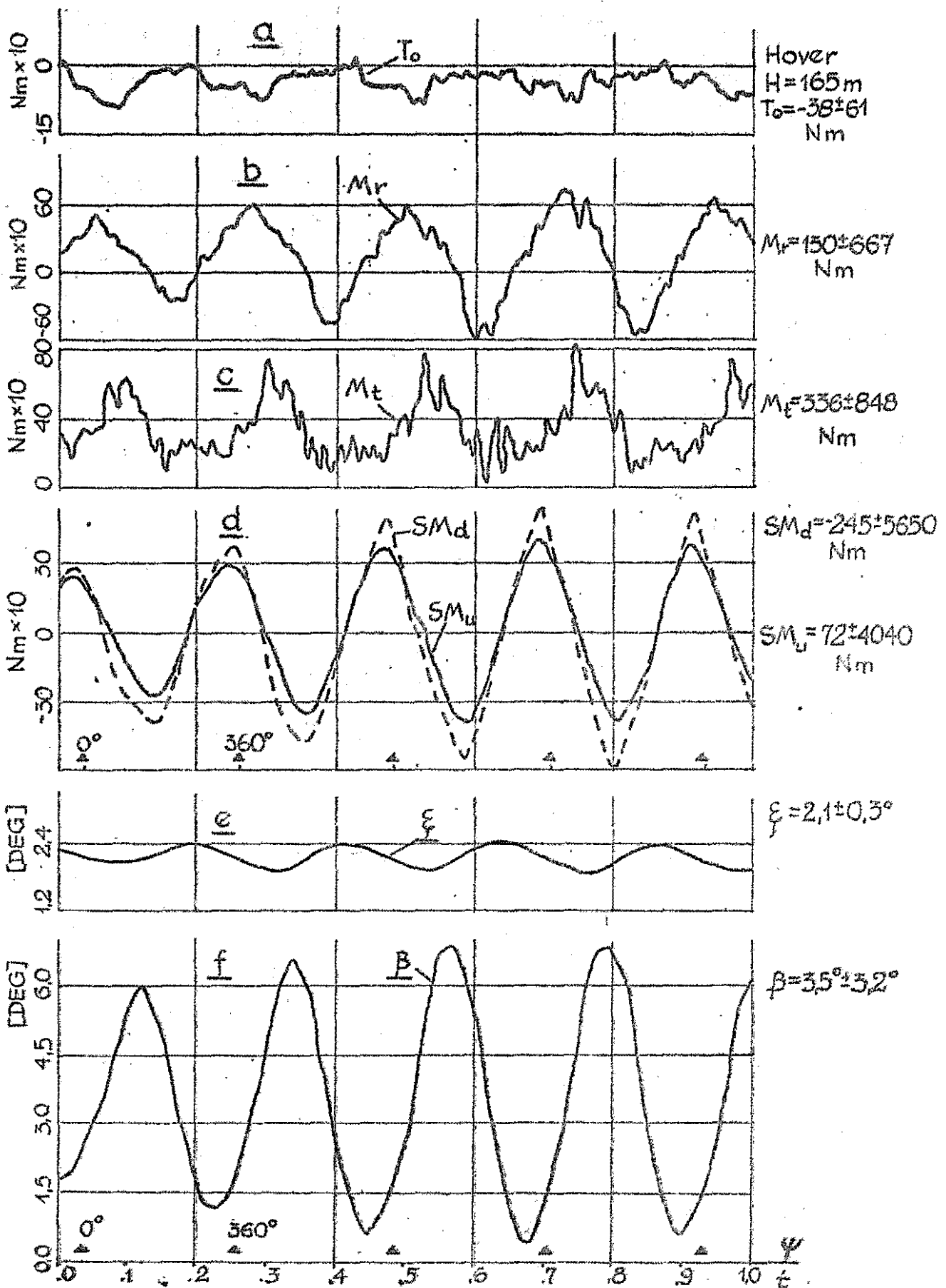


Figure 9. Records of rotor system parameters in hover with wind velocity 28 km/h.  
 $TOM=5410\text{ kg}$ ,  $OAT=29^\circ\text{C}$ ,  $QR=220\text{ m/s}$   
 Blades - variant  $C^*$  with one tab  $8^\circ$  up/at  $\tau=0,867\div 0,925$

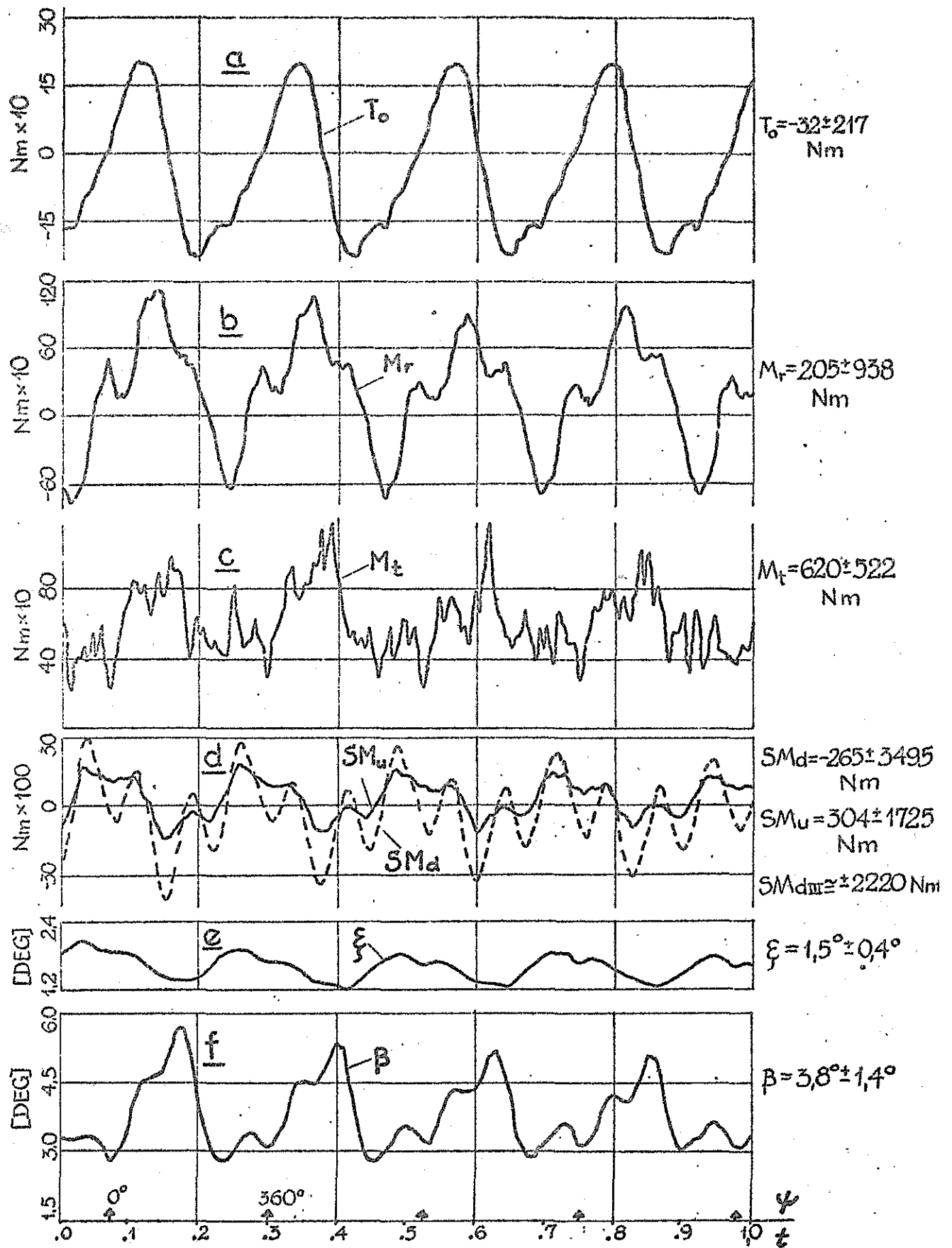


Figure 10. Records of rotor system parameters at level flight with  $V = 206$  km/h.  $TOM = 5410$  kg,  $H = 562$  m,  $OAT = 26^\circ C$ ,  $\Omega R = 217$  m/s. Blades - variant C\*, with one tab  $8^\circ$  up/at  $\bar{r} = 0.867 \div 0.925$

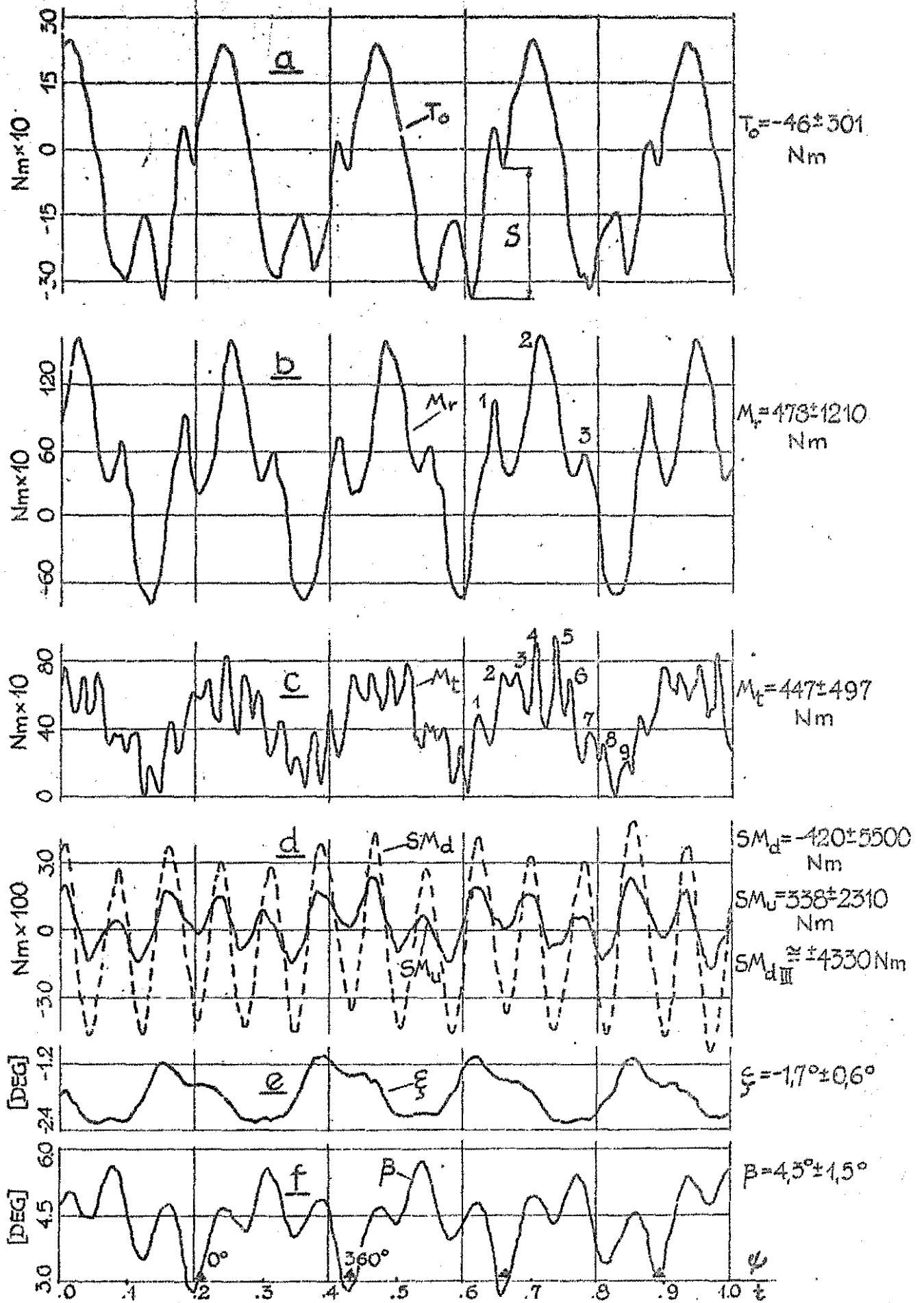


Figure 11. Records of rotor system parameters at level flight with  $V=260$  km/h,  $TOM=5410$  kg,  $H=606$  m,  $OAT=26^\circ C$ ,  $QR=212,5$  m/s. Blades-variant C\* with one tab  $8^\circ$  up/at  $\bar{r}=0,867 \div 0,925$



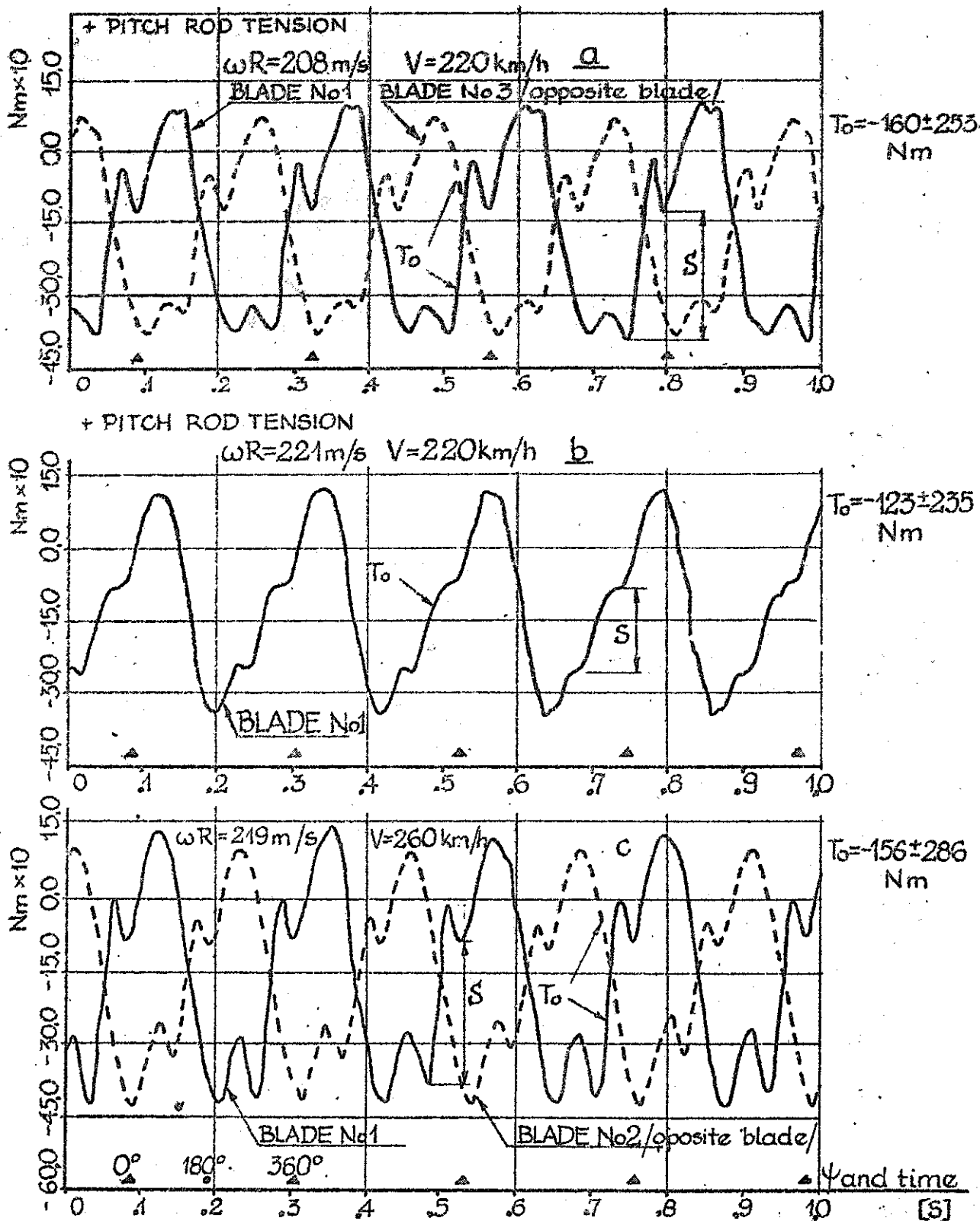


FIGURE 12. RECORDS OF TORSIONAL MOMENTS  $T_0$  OF THE BLADE  
 WITH DIFFERENT ROTOR TIP SPEEDS.  
 $TOM = 6100 \text{ kg}$ ,  $H = 650 \text{ m}$ ,  $OAT = 25^\circ\text{C}$ .  
 BLADES - MODIFIED VARIANT C\* WITH 5% C TABS,  
 ALL DEFLECTED  $4^\circ$  UP

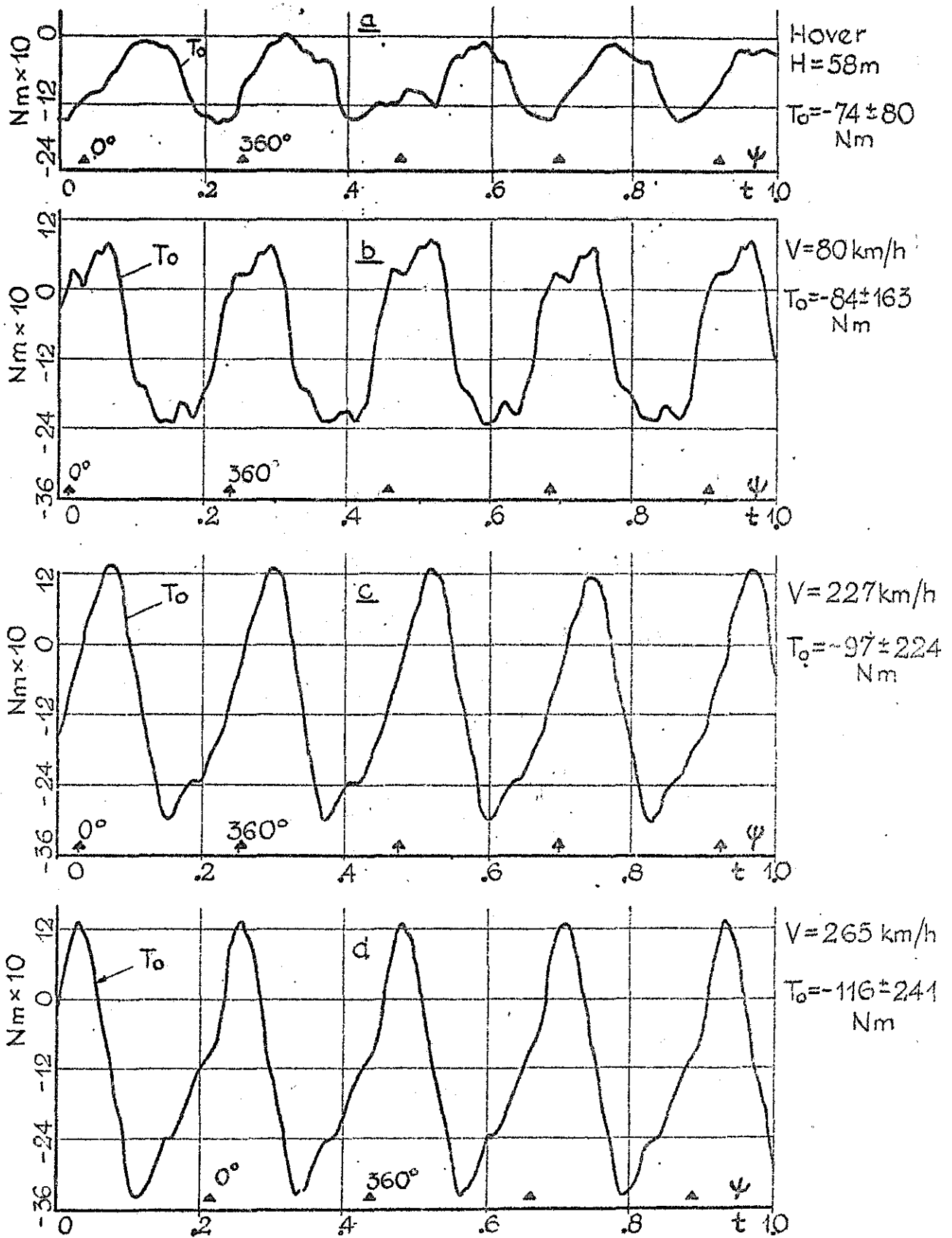


FIGURE 13. RECORDS OF TORSIONAL MOMENTS  $T_0$  OF THE BLADE  
 IN HOVER AND AT DIFFERENT LEVEL AIRSPEEDS  
 $TOM = 6100\text{ kg}$ ,  $H = 440\text{ m}$  /  $OAT = 2^\circ\text{C}$ ,  $\Omega R = 220\text{ m/s}$   
 BLADES - VARIANT C.

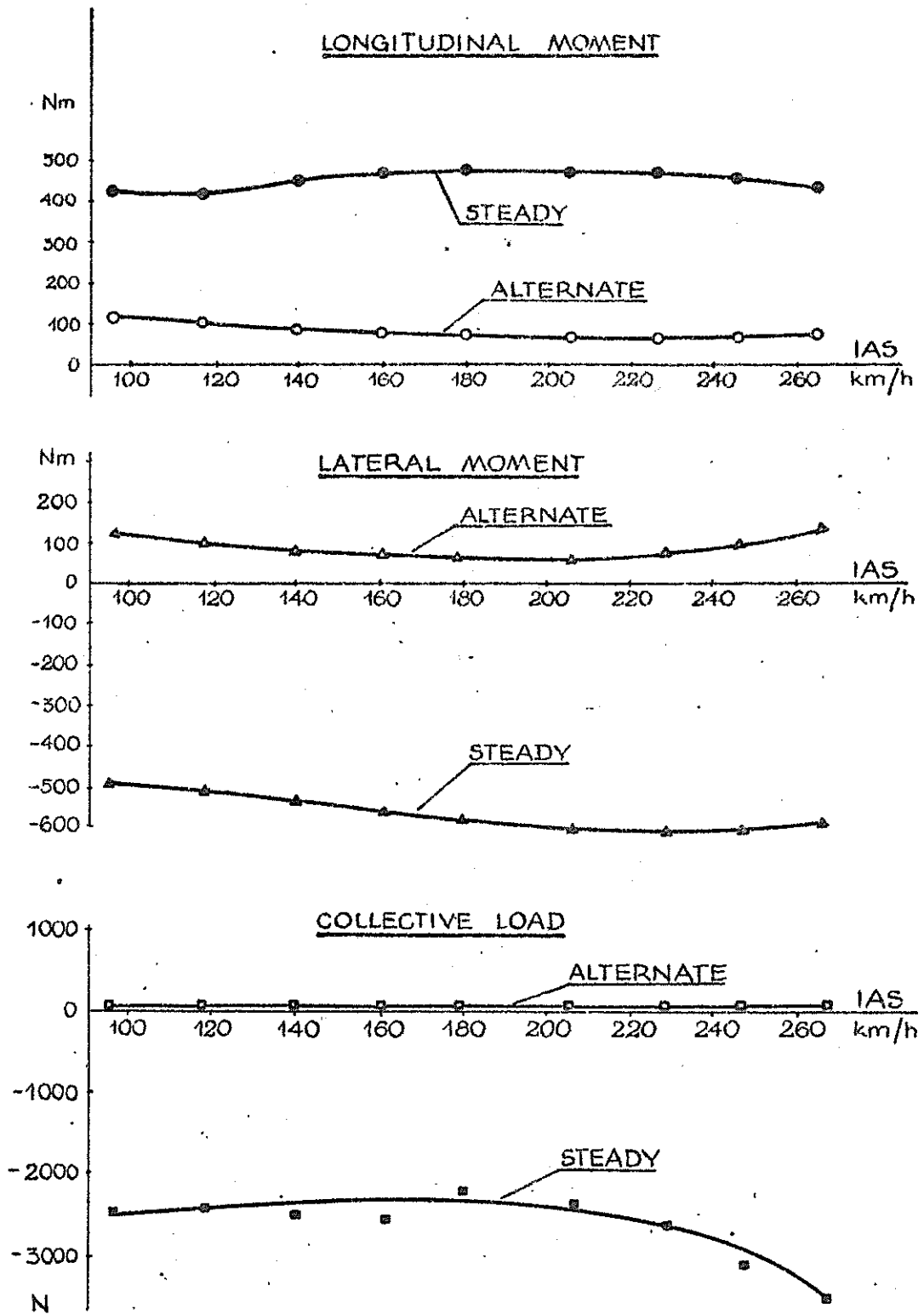


FIGURE 14. SWASHPLATE LOADS VERSUS AIRSPEED,  
 TOM = 6100 kg.  $\Omega R = 220$  m/s. BLADES - VARIANT C.

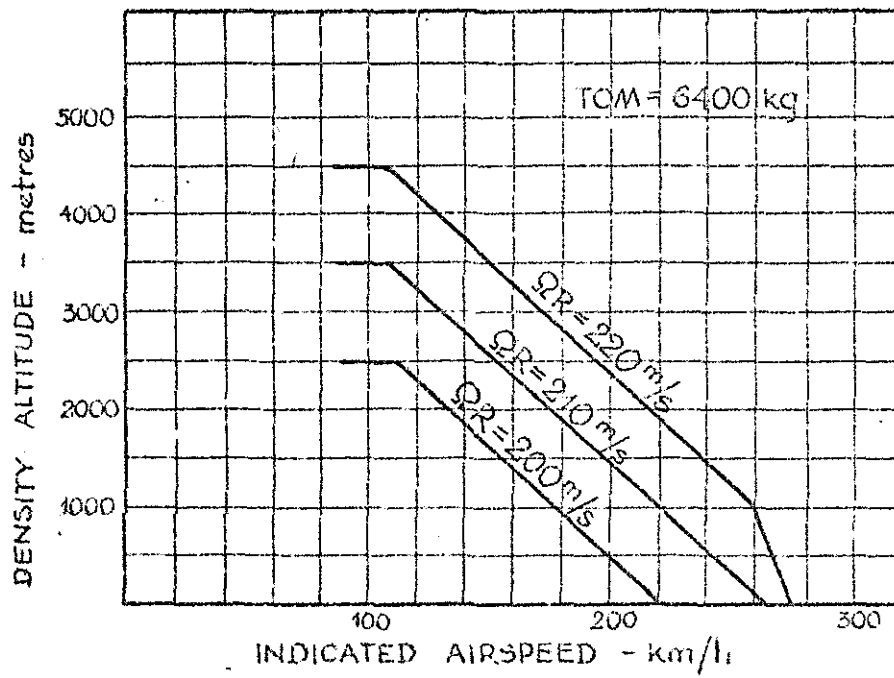
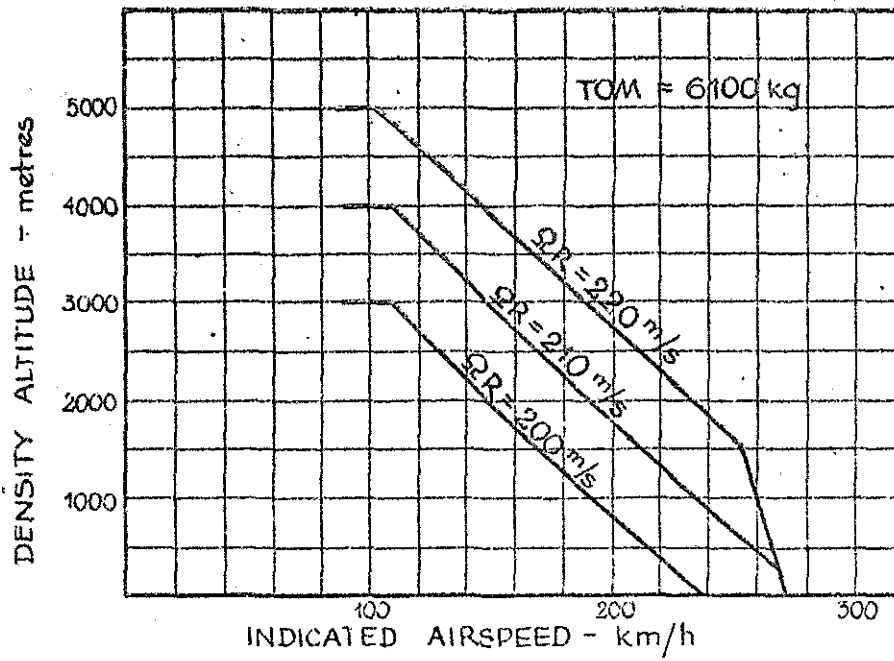


FIGURE 15. MAXIMUM ALLOWABLE AIRSPEED VS DENSITY ALTITUDE AND QR, BLADES - VARIANT C.